Joint arrival-departure taxiway scheduling considering departure uncertainty

Yi Zhang, Yicheng Zhang, Sheng Zhang, Liping Huang and Yifang Yin

Abstract— **The increasing demand for air travel combined with uncertainties has put additional strain on airport infrastructure and ground handling resources. To improve the efficiency of airport operations, in this paper, We firstly perform an in-depth analysis of the A-SMGCS dataset for Singapore Changi Airport, and then propose taxiing routing solutions for both landing and departure aircraft with involved departure uncertainty, formulating the problem as a mixed-integer quadratic programming (MIQP) problem. The proposed model considers the waypoint-based conflict checking, as well as incorporates anti-overtaking constraints, and head-on constraints exclusive for bidirected graph, aiming to minimize the taxiing time as well as the gap with the scheduled in-block time for landing aircraft and scheduled take-off time for departure aircraft. The presence of departure uncertainty prompts us to build a stochastic model, where constraints with stochastic variables are converted into corresponding chance constraints under designated confidence levels. Incorporating stochastic factors enhances the resilience and dependability of our solution. To evaluate the efficiency of our proposed method, we have elaborately investigated the computational complexity under various test scales, and analyzed how changes in uncertainty and confidence levels impact routing and scheduling solutions on a simplified Singapore Changi Airport network, which could provide significant reference for other work.**

Index Terms – airport surface operation, taxiway routing/scheduling, departure uncertainty, stochastic optimization, mixed-integer quadratic programming

I. Introduction

Airports have always been a major bottleneck in air traffic management systems, accounting for most reported Air Traffic Flow Management (ATFM) delays. With the lifting of lockdowns, there is an expected surge in demand for air travel due to "revenge travel," as passengers who have been unable to travel during the pandemic seek to make up for lost time [6]. This phenomenon will exacerbate the growth of air travel, which has also led to challenges such as congested airports, capacity bottlenecks, and increased costs for airlines. One potential solution to address this issue is to optimize the use of airport surface resources such as taxiways, which are critical to improving the efficiency of the airport surface operation [2].

Airport taxiway operation involves routing and scheduling aircraft while prioritizing safety and minimizing travel time. For smaller airports with few aircraft, shortest path algorithms, such as Dijkstra's algorithm, are suitable for dealing with few conflicts [10]. However, larger airports with more aircraft require simultaneous routing algorithms. Both optimization and simulation approaches have been proposed in existing research. Adacher et al. develop an algorithm that firstly assigns routes to each aircraft and then formulate a job-shop scheduling problem based on the selected route [1] to minimize both taxiing delay and pollution emissions. By integrating taxiway and runway operations, Yu Jiang et al. propose a mixed-integer linear programming (MILP) problem [5], with the aim to reduce the total taxiing route length and waiting delay time. However, their improved genetic algorithm for dealing with large computation challenges was tested on a simplified network without considering the gate waypoints. With a similar model framework following the continuous time fashion, Soltani et al. propose a conflict-free MILP model targeting on taxiways and incorporate the assignment of electric vehicles for towing operation to minimize the fuel consumption [9]. The model is solved by the optimization solver CPLEX [3] and tested on Montreal's Pierre Elliott Trudeau airport, consisting of 141 waypoints. To address the problem's size, a rolling-horizon approach was employed to assist in finding a solution.

Airdrome surface operation is subject to various uncertainties arising from factors such as severe weather conditions, emergencies, fluctuations in flight speed, changes in network capacity, and so on. However, existing studies have mainly focused on optimizing various deterministic operations, but seldom strategic decision-making studies have yet considered the uncertainty existing in the surface network, only some studies on enroute traffic [7][8]. Therefore, we propose this work to provide taxiing routing solutions for both landing and departure aircraft with involved departure uncertainty. We formulate the problem as a mixed-integer quadratic programming (MIQP) problem, taking the safety separation into account, e.g., node conflict constraints, anti-overtaking constraints, and head-on constraints, with the aim to minimize the taxiing time as well as the gap with the scheduled in-block time for landing aircraft and scheduled take-off time for departure aircraft. The departure uncertainty from departure aircraft enables mixed-mode constraints in our modelling, which leads to 3 modes in all safety-checking constraints. In the simulation, we test the computational complexity of the proposed model under test cases with various scales. Also, we investigate how routing and scheduling are impacted by the change of the uncertainty and confidence levels.

The content of this paper is organized as follows. Section II analyses the departure uncertainty in one day A-SMGCS dataset. Section III illustrates the detailed formulation of our

Yi Zhang, Yicheng Zhang, Sheng Zhang, Liping Huang and Yifang Yin are with the Institute for Infocomm Research (I^2R), Agency for Science, Technology and Research (A*STAR), 1 Fusionopolis Way, #21-01 Connexis, Singapore 138632, Republic of Singapore. Emails: yzhang120@e.ntu.edu.sg (zhang_yi@i2r.a-star.edu.sg), yzhang088@e.ntu.edu.sg (zhang_yicheng@i2r.a-star.edu.sg), szhang034@e.ntu.edu.sg (zhang_sheng@i2r.a-star.edu.sg), huang_liping@i2r.a-star.edu.sg, yifangyin99@gmail.com (yin_yifang@i2r.a-star.edu.sg)

This work is supported by the National Research Foundation, Singapore, and the Civil Aviation Authority of Singapore (CAAS), under the Aviation Transformation Programme. (Grant No. ATP_IOP for ATM_I2R_2)

proposed optimization model. Next, Section IV describes the experimental results on computational complexity and impacts of the uncertainty. Finally, conclusions are draw in Section V.

II. Airport data analysis

In order to verify the existence of the departure uncertainty in airdrome, we conduct the data analysis using one-day A-SMGCS (Advanced Surface Movement Guidance and Control System) data for Singapore Changi Airport. We observed one day departure aircraft trajectory data at October 22, 2019, where a total of 435 aircraft with more than 500 thousand records are extracted, with information such as epoch time, aircraft callsign, aircraft type, latitude and longitude position. A-SMGCS provides the real history data, in order to check departure uncertainty, we also obtained the scheduled flight plan at the same day, which provides information such as departure airport, aircraft callsign, scheduled off-block time (SOBT).

Although A-SMGCS data adopts hybrid sensors, e.g., radar, ADS-B, camera, to improve accuracy, missing data points still exist in the original dataset, thus, we conduct linear interpolation for the missing latitude and longitude due to the straight characteristics of taxiways. Next, speed is calculated with a 60-second difference gap to reduce the high variance and keep a smooth speed curve. After that, the actual off-block time (AOBT) is determined when the aircraft speed firstly reaches 5 knots. The extracted AOBT is merged with the SOBT in flight plan based on the aircraft callsign. Then the histogram of time differences between AOBT and SOBT is drawn in Fig. 1. Clearly, the majority of aircraft do not depart on time, with a significant number being delayed between 0 and 15 minutes. Based on this, we propose our optimized solutions for airdrome aircraft scheduling and routing incorporated with the departure uncertainty in next section.

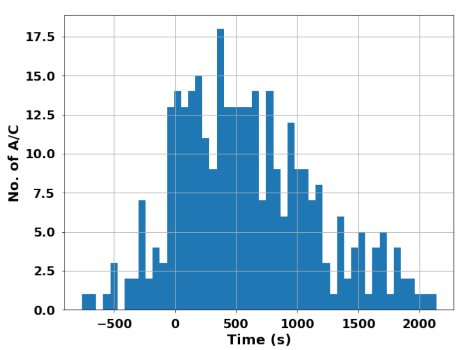

Fig. 1: The difference distribution between AOBT and SOBT

III. Model Formulation

The taxiing scheduling model is defined on a bidirected graph (except few edges, such as runway exits/entrances), with $\mathcal{G} = \{\mathcal{N}, \mathcal{L}\}$, where $\mathcal{N}$ denotes the taxiway nodes/waypoints, and $\mathcal{L}$ denotes the edge segments between any two waypoints. $\mathcal{N}_r \in \mathcal{N}$ denotes the runway exit/entrance waypoints, $\mathcal{N}_a \in \mathcal{N}$ denotes the gate waypoints. $\mathcal{F}$ is the entire aircraft set, where $\mathcal{F}_a \in \mathcal{F}$ denotes the arrival aircraft, $\mathcal{F}_d \in \mathcal{F}$ denotes the departure aircraft. In the following formulated model, we only consider the uncertainty for departure aircraft, this is because we assume the landing time is our inputs and our control is from the surface perspective, treating the landing time of arrival aircraft the same way as departure aircraft would require the cooperation from the airborne side, which is not integrated in current framework.

1) Node conflict checking: A safety gap T_{min} must be met when any two aircraft is approaching the same node j. This can be formulated as constraints (1): either aircraft f arrive earlier than $f^{'}$ or vice versa. We define t_i^f ($\tilde{t}_i^f$) as the deterministic (stochastic) arrival time of aircraft f at waypoint i. δ_i^f is the arrival time uncertainty for aircraft f at waypoint i. x_{ij}^f is the binary variable for route selection. Due to the existence of departure uncertainty, arrival time variables become stochastic variables, $\tilde{t}_i^f$, for all departure aircraft, while the arrival time for landing aircraft, t_i^f, belongs to the deterministic domain, accordingly, we will have three modes based on the aircraft types, depicted as follows:

$$\forall i, j \in \mathcal{N} : \sum_i x_{ij}^f = 1 \wedge \sum_i x_{ij}^{f^{'}} = 1 \rightarrow$$

$$\textbf{\textit{mode I:}} \quad \forall f, f^{'} \in \mathcal{F}_a,$$

$$\text{either } (t_j^f + T_{min} \leq t_j^{f^{'}}) \text{ or } (t_j^{f^{'}} + T_{min} \leq t_j^f) \tag{1a}$$

$$\textbf{\textit{mode II:}} \quad \forall f \in \mathcal{F}_d, f^{'} \in \mathcal{F}_a,$$

$$\text{either } (\tilde{t}_j^f + T_{min} \leq t_j^{f^{'}}) \text{ or } (t_j^{f^{'}} + T_{min} \leq \tilde{t}_j^f) \tag{1b}$$

$$\textbf{\textit{mode III:}} \quad \forall f, f^{'} \in \mathcal{F}_d,$$

$$\text{either } (\tilde{t}_j^f + T_{min} \leq \tilde{t}_j^{f^{'}}) \text{ or } (\tilde{t}_j^{f^{'}} + T_{min} \leq \tilde{t}_j^f) \tag{1c}$$

As stochastic variables exist in the constraints (1b) and (1c), which can be converted to a chance constraint with probability α. As the derivation about both constraints (1b) and (1c) is similar, the following inequalities only illustrate the derivation process for the left logic constraint of (1c) under the probability function P.

$$P((t_j^f + \delta_j^f) + T_{min} \leq (t_j^{f^{'}} + \delta_j^{f^{'}})) \geq \alpha \tag{2a}$$

$$P(\delta_j^f - \delta_j^{f^{'}} \leq t_j^{f^{'}} - t_j^f - T_{min}) \geq \alpha \tag{2b}$$

Inequality constraints (2) can be converted into a linear constraint by the cumulative distribution function (CDF), $\mathcal{F}$, of $\delta_j^f - \delta_j^{f^{'}}$ and evaluated at $t_j^{f^{'}} - t_j^f - T_{min}$. Accordingly, we have

$$\mathcal{F}_{\delta_j^f - \delta_j^{f^{'}}}(t_j^{f^{'}} - t_j^f - T_{min}) \geq \alpha \tag{3a}$$

$$t_j^{f^{'}} - t_j^f - T_{min} \geq \mathcal{F}^{-1}_{\delta_j^f - \delta_j^{f^{'}}}(\alpha) \tag{3b}$$

where $\mathcal{F}^{-1}_{\delta_j^f - \delta_j^{f^{'}}}(\alpha)$ is the inverse of CDF, which represents the value of the random variable $\delta_j^f - \delta_j^{f^{'}}$ such that the probability of the difference being less than or equal to that value is α. In other words, it gives us the value of $t_j^{f^{'}} - t_j^f - T_{min}$ such that the probability of the difference in arrival time uncertainty being less than or equal to that value is α. Since we assume only normal distribution is considered in this paper, we have $\delta_j^f \sim N(\mu_j^f, \sigma_j^{f^2})$ and $\delta_j^{f'} \sim N(\mu_j^{f'}, \sigma_j^{f'^2})$, then we can obtain $(\delta_j^f - \delta_j^{f'}) \sim N(\mu_j^f - \mu_j^{f'}, \sigma_j^{f^2} + \sigma_j^{f'^2})$. Given the confidence level α and normal distribution, we can obtain the confidence interval $\mathcal{F}^{-1}_{\delta_j^f - \delta_j^{f'}}(\alpha)$, accordingly, constraint (3b) becomes a linear constraint.

2) Rear-end conflict checking - anti-overtaking: When any two aircraft pass by the same edge ij, we do not allow the over-taking behaviour. Accordingly, if both aircraft f and f' pass by the edge ij, and aircraft f arrives at node i earlier than aircraft f', then aircraft f must leave node j earlier than aircraft f', meanwhile guarantee the safety gap T_{min}.

$$\forall i, j \in \mathcal{N} : x_{ij}^f = 1 \wedge x_{ij}^{f'} = 1 \rightarrow$$

$$\textbf{\textit{mode I:}} \quad \forall f, f' \in \mathcal{F}_a,$$

$$\text{if } (t_i^f \leq t_i^{f'}) \rightarrow (t_j^f + T_{min} \leq t_j^{f'}) \tag{4a}$$

$$\text{if } (t_i^{f'} \leq t_i^f) \rightarrow (t_j^{f'} + T_{min} \leq t_j^f) \tag{4b}$$

$$\textbf{\textit{mode II:}} \quad \forall f \in \mathcal{F}_d, f' \in \mathcal{F}_a,$$

$$\text{if } (\tilde{t}_i^f \leq t_i^{f'}) \rightarrow (\tilde{t}_j^f + T_{min} \leq t_j^{f'}) \tag{4c}$$

$$\text{if } (t_i^{f'} \leq \tilde{t}_i^f) \rightarrow (t_j^{f'} + T_{min} \leq \tilde{t}_j^f) \tag{4d}$$

$$\textbf{\textit{mode III:}} \quad \forall f, f' \in \mathcal{F}_d,$$

$$\text{if } (\tilde{t}_i^f \leq \tilde{t}_i^{f'}) \rightarrow (\tilde{t}_j^f + T_{min} \leq \tilde{t}_j^{f'}) \tag{4e}$$

$$\text{if } (\tilde{t}_i^{f'} \leq \tilde{t}_i^f) \rightarrow (\tilde{t}_j^{f'} + T_{min} \leq \tilde{t}_j^f) \tag{4f}$$

Similar to the deviation in subsection III-.1, we can convert the above constraints (4c) - (4f) with stochastic variables to its corresponding linear constraints.The deviation process is omitted due to the page limitation.

3) Head-on conflict checking: Taxiway normally follows a bidirectional fashion to increase efficiency and reduce congestion in busy airports. Thus, when two aircraft is heading towards each other, we need to guarantee that each edge can only be visited by one aircraft at each time: when aircraft f needs to travel edge ij and aircraft f' needs to travel edge ji, then either f leaves node j first or f' finishes node i first, which can be illustrated as follows:

$$\forall i, j \in \mathcal{N} : x_{ij}^f = 1 \wedge x_{ji}^{f'} = 1 \rightarrow$$

$$\textbf{\textit{mode I:}} \quad \forall f, f' \in \mathcal{F}_a,$$

$$\text{either } (t_j^f + T_{min} \leq t_j^{f'}) \text{ or } (t_i^{f'} + T_{min} \leq t_i^f) \tag{5a}$$

$$\textbf{\textit{mode II:}} \quad \forall f \in \mathcal{F}_d, f' \in \mathcal{F}_a,$$

$$\text{either } (\tilde{t}_j^f + T_{min} \leq t_j^{f'}) \text{ or } (t_i^{f'} + T_{min} \leq \tilde{t}_i^f) \tag{5b}$$

$$\textbf{\textit{mode III:}} \quad \forall f, f' \in \mathcal{F}_d,$$

$$\text{either } (\tilde{t}_j^f + T_{min} \leq \tilde{t}_j^{f'}) \text{ or } (\tilde{t}_i^{f'} + T_{min} \leq \tilde{t}_i^f) \tag{5c}$$

Similarly, the above constraints can be converted to the chance constraints, we omit the process due to the page limitation.

4) Arrival time constraints: As long as an edge ij is selected as part of the route, the arrival time at downstream node j is updated by the travel time and the arrival time at upstream node i, where we depict the travel time by the distance d_{ij} and the reciprocal of the speed R_{ij}^f.

$$\forall f \in \mathcal{F}, i, j \in \mathcal{N} :$$

$$x_{ij}^f = 1 \rightarrow t_j^f = t_i^f + d_{ij} R_{ij}^f \tag{6a}$$

$$\frac{1}{v_{max}} \leq R_{ij}^f \leq \frac{1}{v_{min}} \tag{6b}$$

Also, as our control is from the taxiway's perspective, the landing time is the inputs of our model, as illustrated in constraint (7a). On the other hand, the departure time can be considered as one of the decision variable within a range of $SOBT$, as depicted in constraint (7b).

$$\forall f \in \mathcal{F}_a, i \in \mathcal{N}_r, j \in \mathcal{N} :$$

$$\sum_j x_{ij}^f = 1 \rightarrow t_i^f = ATA_f \tag{7a}$$

$$\forall f \in \mathcal{F}_d, i \in \mathcal{N}_a, j \in \mathcal{N} :$$

$$\sum_j x_{ij}^f = 1 \rightarrow SOBT_f - \gamma \leq t_i^f \leq SOBT_f + \gamma \tag{7b}$$

5) Route selection constraints: At the beginning, we need to know which aircraft, either landing or departure, starts taxiing from which waypoint. If aircraft f starts at node i, then the parameter AS_i^f becomes 1, otherwise, it is zero, and this parameter is assigned to the route variable to label the start location.

$$\forall f \in \mathcal{F}_a, i \in \mathcal{N}_r, j \in \mathcal{N} : \sum_j x_{ij}^f = AS_i^f \tag{8a}$$

$$\forall f \in \mathcal{F}_d, i \in \mathcal{N}_a, j \in \mathcal{N} : \sum_j x_{ij}^f = AS_i^f \tag{8b}$$

In the middle, we need to keep the conservation law through the whole route, namely, the sum of route variables from all upstream nodes towards current node j must equal to the sum of route variables towards all downstream nodes from node j. Also, whether edge ij can be selected or not depends on the adjacent matrix ADJ.

$$\forall f \in \mathcal{F}, i, j, q \in \mathcal{N} : \sum_i x_{ij}^f = \sum_q x_{jq}^f \tag{9a}$$

$$\forall f \in \mathcal{F}, i, j \in \mathcal{N} : x_{ij}^f \leq ADJ_{ij} \tag{9b}$$

For the sink part, each landing (departure) aircraft must be assigned to an gate (runway entrance) node, namely, the sum of route variables towards all gate nodes from all upstream nodes for all landing aircraft f must equal to the number of assignments for landing aircraft, similar to departure aircraft, which are illustrated in constraints (10a) and (10b) below.

$$\sum_{f \in \mathcal{F}_a} \sum_{i \in \mathcal{N}} \sum_{j \in \mathcal{N}_a} x_{ij}^f = \sum_{f \in \mathcal{F}_a} \sum_{i \in \mathcal{N}_r} AS_i^f \tag{10a}$$

$$\sum_{f \in \mathcal{F}_d} \sum_{i \in \mathcal{N}} \sum_{j \in \mathcal{N}_r} x_{ij}^f = \sum_{f \in \mathcal{F}_d} \sum_{i \in \mathcal{N}_a} AS_i^f \tag{10b}$$

$$\forall j \in \mathcal{N}_a, \sum_{f \in \mathcal{F}_a} \sum_{i \in \mathcal{N}} x_{ij}^f \leq 1 \tag{10c}$$

Also, constraint (10c) indicates that only one landing aircraft can be parked at each gate node.

6) Objective function: The whole system is trying to minimize the sum of gate in-block gap, runway take-off gap and total taxiing time, which is illustrated as follows:

$$J = \sum_{f\in\mathcal{F}^a}\sum_{i\in\mathcal{N}_a}(t_i^f - SIBT_f)^2 + \sum_{f\in\mathcal{F}^d}\sum_{i\in\mathcal{N}_r}(t_i^f - STOT_f)^2 + \sum_{f\in\mathcal{F}^a}(\sum_{i\in\mathcal{N}_a} t_i^f - \sum_{i\in\mathcal{N}_r} t_i^f AS_i^f) + \sum_{f\in\mathcal{F}^d}(\sum_{i\in\mathcal{N}_r} t_i^f - \sum_{i\in\mathcal{N}_a} t_i^f AS_i^f) \tag{11}$$

where ATA is the actual time of arrival, $SOBT$ is the scheduled off-block time, $SIBT$ is the scheduled in-block time, and $STOT$ is the scheduled take-off time. $\sum_{f\in\mathcal{F}^a}\sum_{i\in\mathcal{N}_r} t_i^f AS_i^f$ and $\sum_{f\in\mathcal{F}^d}\sum_{i\in\mathcal{N}_a} t_i^f AS_i^f$ depict the sum of the landing time of arrival aircraft at all runway exit nodes and the sum of leaving time of all departure aircraft at all gate nodes, respectively.

IV. Simulation Results

A. Computational complexity

Even though the above constraints with stochastic variables are converted into linear chance constraints with corresponding inverse CDF, the logic still exists, thus, big-M method is adopted to convert them as a mixed-integer quadratic programming (MIQP) problem, which is then coded in python and solved by the commercial solver Gurobi [4]. The programming code is running on a PC with 12th Gen Intel(R) Core(TM) i7-12700H * 20 CPU up to 4.70 GHz and RAM 16GB. To investigate the proposed model, we initially consider a partial Singapore Changi airport, which has total of 28 gates for Terminal 3, 51 taxiway intersections and 2 entrances and 3 exits for runway 02L. Even though we have only considered apron parking area of Terminal 3 for a total of 84 waypoints, the network is still very complex for a model involved uncertainty. Also, the intention of this paper is to investigate the impacts of the departure uncertainty, thus, we simplify the original network to a network with 49 waypoints, as illustrated in Fig. 2, where red, orange, green and light blue waypoints illustrate the runway entrances, runway exits, gate parking and intermediate taxiing intersections, respectively. To investigate the model complexity, we have

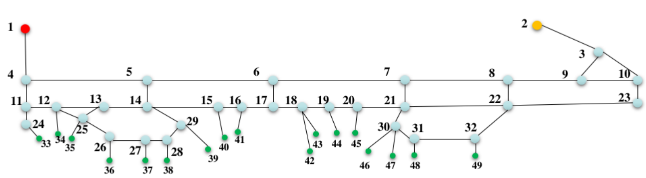

Fig. 2: Simplified Taxiway Layout

summarized 10 cases under different number of aircraft, as illustrated in Table I, where N^f, N_a^f, N_d^f, N_{cons}, N_{vars} and α denote the number of aircraft, arrival (landing) aircraft, departure aircraft, constraints, variables and confidence level, respectively. The larger the value of α, the harder the chance constraint. When the number of taxiing aircraft is high, the solution domain will be reduced. Therefore, we set lower α value for larger cases. ATA and $SOBT$ of each aircraft is randomly generated within one hour for all 10 cases. $SIBT$ and $STOT$ are obtained by the ideal 15-minute summation on ATA and $SOBT$, respectively. The uncertainty of departure follows $\delta_i^f \sim$ N(0, 300). The speed range is given between 5 km/h and 60 km/h.

TABLE I: Test cases under different parameter settings

Cases	N^f	N_a^f	N_d^f	N_{cons}	N_{vars}	α
Case 1	5	2	3	100221	37925	70%
Case 2	10	3	7	445413	138310	70%
Case 3	10	5	5	445437	138340	70%
Case 4	10	7	3	445461	138370	70%
Case 5	15	5	10	1035617	301185	70%
Case 6	15	7	8	1035641	301215	70%
Case 7	15	10	5	1035677	301260	70%
Case 8	18	7	11	1507349	428910	50%
Case 9	20	10	10	1870857	526580	50%
Case 10	20	12	8	1870881	526610	50%

By checking Table I, we can find that the problem scale increases as the increase of the aircraft number. The reason why larger arrival aircraft number introduces more constraints and variables is because the additional constraint (10c) targeting for landing aircraft. Also, when the total number of aircraft becomes 15, the scale of constraints has reached the million level. Luckily, Gurobi has the presolve function to reshape the model to eliminate the extra constraints and variables, such as the non-connectivity edge in our model. The scale of the presolved model is listed in Table II. Clearly, the computational time exponentially increases as the increase of the problem scale: Case 8 has roughly 10^+ times of Case 1 for either original or presolved model, but the computation time of Case 8 is already 10 thousand times larger than Case 1. Even Case 10 fails to obtain the results given a time limit of 8 hours. Another noteworthy aspect is that the change of the computational time does not strictly follow the scale of the presolved model but the original model, e.g., the scale of the presolve model of Case 8 is smaller than Case 7 but with a much larger computation time. Thus, the computation time is not only driven by the problem scale but also impacted by the feasible solution domain: the newly added 6 departure aircraft with uncertainty introduces more complexity compared to the relief provided from the removal of 3 deterministic arrivals. We also list out the results of each item of the objective cost J, namely, gate in-block gap, runway take-off gap, and taxiing time of arrival and departure aircraft. As a preliminary study of departure uncertainty, we didn't provide different weights on these objects, which shall be studied in our future work to assess the impact of different stakeholders and quantify their contributions. The interesting part is that every aircraft is capable of taking off or landing at its designated gate at the scheduled time, and this may be due to the small deviation, 300 s, we selected for σ_j^f, and the confidence levels, which has been decreased to 50% for last 3 larger cases. In the next subsection, we will observe how this behavior changes as we modify the confidence level and σ_j^f. Also, the taxiing time of arrival aircraft is normally larger than that of departure aircraft, this is because the runway landing time, ATA_f, is directly assigned to each aircraft, as depicted in constraint (7a), while the departure time is within a range of the scheduled off-block time $SOBT_f$ in constraint (7b), thus, departure aircraft has more flexibility to shrink their taxiing time.

B. Impacts of confidence level and uncertainty

To investigate the impacts of confidence levels and uncertainties, we select the same inputs as Case 2, with 3 arrival aircraft and 7 departure aircraft, and speed range between 10 km/h and 60 km/h. Fig. 3 illustrates the runway take-off gap, arrival aircraft taxiing time and departure aircraft taxiing time for 4 different confidence levels α, from 60% to 90%. As the gate in-block times are all 0 for 4 different cases, they are not shown in the figure. Obviously, the total cost J increases as the increase of the value α. The costs for 60% and 70% are the same for taxiing times of departure and arrival aircraft, and all arrival and departure aircraft reaches their destinations at the designated time. However, runway take-off gap starts to have value when α increases to 80%, also, both take-off gap and departure aircraft taxiing time significantly increases when α reaches to 90%. The reason why take-off gap starts to increase instead of the in-block time gap is because we have more gate nodes to select for arrival aircraft compared with the one single runway exit node for departure aircraft. Moreover, the small upper right figure shows the computational time under each confidence level, clearly, with the increase of the confidence level, the computational time exponentially increases.

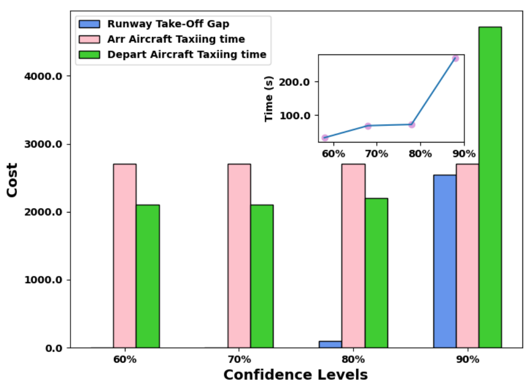

Fig. 3: Costs and computation time under different confidence levels

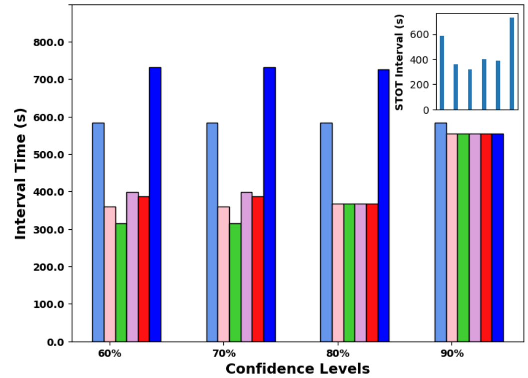

Fig. 4: Take-off intervals for departure aircraft at runway exit node under different confidence levels

Fig. 4 illustrates the intervals of aircraft take-off times, $t_i^f - t_i^{f'}$, at runway exit between adjacent departure aircraft under different confidence levels. The upper right small figure shows the STOT interval time ($STOT_f - STOT_{f'}$) for 7 departure aircraft. Clearly, intervals under 60% and 70% have the same shape as the STOT intervals of the small figure, namely, all aircraft reaches runway exit node at the designated STOT time, accordingly, leads to 0 runway take-off gap time ($t_i^f - STOT_f$) in Fig. 3. However, as the confidence level increases, the lower bound of interval time also increases: from 316 under 60% and 70%, 367 under 80% towards 553 under 90%.

To investigate the impacts of different uncertainties, we use the same inputs with 3 arrival aircraft and 7 departure aircraft, and tested on 3 different settings of σ_i^f, namely, 5 min, 10 min and 15 min. Fig. 5 illustrates the time-space diagram depicting the movements of departure aircraft under 3 different uncertainties. The waypoint index is arranged to step down the y coordinates, from 49 to 1. Thus, the slope of the line shown in the Fig. 5 does not represent the real speed. In the figure, there are no instances of two aircraft sharing the same link while violating the conflict constraints. In Fig. 5a, some departure aircraft detour a little bit in order to meet the STOT at runway exit. However, all aircraft start to detour when σ becomes 10-min, larger σ value leads to larger safety gap for any two aircraft, accordingly, we can find that the time interval between adjacent trajectories at final runway exit, 1, has become increasingly larger, especially for a deviation of 15 minutes, whose ticks on x-axis have already reach 5000. Even though we provide flexibility on off-block time for departure aircraft, constraint (7b), almost all departure aircraft starts taxiing at $SOBT + \gamma$, even so, aircraft still needs to detour to guarantee the enlarged gap. The reason why aircraft f_5 starts earlier in Fig. 5b and 5c is because there is another arrival aircraft needs to occupy edge 8-7 around 1600s, thus, f_5 starts earlier to avoid conflict at node 7. Also, in order to reach node 6 at around 2600s to maintain the safety gap at the final several segments, aircraft f_7 starts earlier and takes a detour to meet the time, otherwise, wait till final allowed off-block time ($SOBT+\gamma$) and directly travel from node 46 to 6 via other paths, would be earlier even if the slowest speed 10 km/h is selected.

V. Conclusion

In this paper, we firstly conduct a detailed data analysis on A-SMGCS dataset for Singapore Changi Airport, in order to verify the existence of the depature uncertainty. Next, we propose a stochastic optimization model for both landing and departure aircraft by incorporating the departure uncertainty, which is formulated as a MIQP problem, with the aim to minimize taxiing time and the gap with SIBT and STOT, respectively. In the simulation test, we investigate the computational complexity of the model under various problem scales, which indicates that the compute time increases exponentially as the increase of the problem scale. Also, by testing on different deviation bounds and confidence levels, we have found that the larger the deviation (or the higher

TABLE II: Computational times and objective costs for 10 cases

	N^P_{cons}	N^P_{vars}	**Computational Time (s)**	**Objective Cost J**	**Gate In-block Gap**	**Runway Take-Off Gap**	**Arr Aircraft Taxiing Time**	**Depart Aircraft Taxiing Time**
Case 1	6018	2648	1.0140	2700	0	0	1800	900
Case 2	22922	8956	13.1077	4800	0	0	2700	2100
Case 3	88241	17128	14.3483	6000	0	0	4500	1500
Case 4	73411	16076	155.371	7200	0	0	6300	900
Case 5	51951	19450	314.253	7490	0	0	4490	3000
Case 6	80715	22201	420.777	8700	0	0	6300	2400
Case 7	151232	31690	4803.67	10500	0	0	9000	1500
Case 8	78643	29272	10523.8	9600	0	0	6300	3300
Case 9	139830	40969	23771.3	12000	0	0	9000	3000
Case 10	344509	60576	⋆	⋆	⋆	⋆	⋆	⋆

⋆ means Gurobi fails to generate results after running 8 hours.

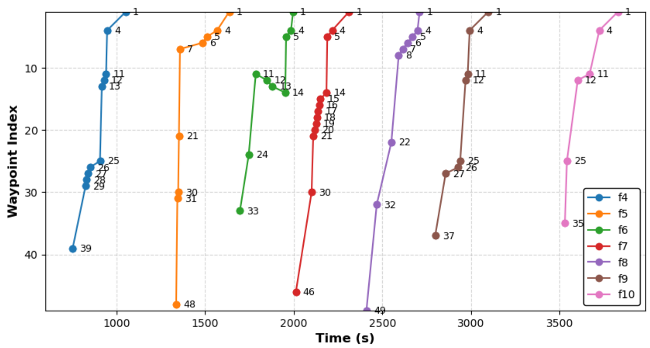

(a) 5-min Deviation

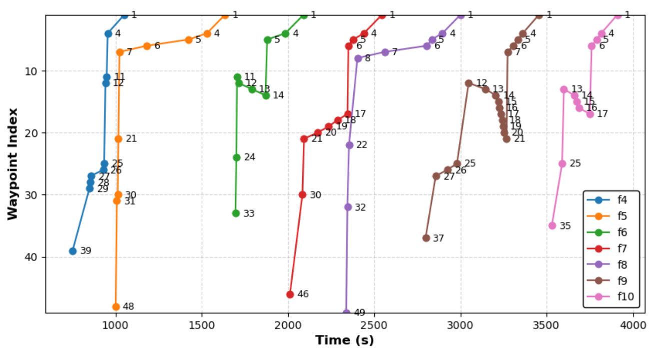

(b) 10-min Deviation

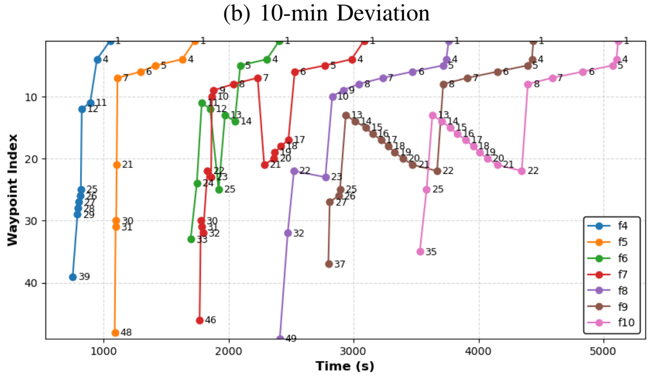

(c) 15-min Deviation

Fig. 5: Taxiing trajectory for departure aircraft under different uncertainties

the confidence level), the more difficult to find the optimal result, and the large cost value the objective, as well as more detour occurrences for departure aircraft.

ACKNOWLEDGEMENT

The authors would like to thank all colleagues from CAAS for providing valuable comments and suggestions on this work. Any opinions, findings and conclusions or recommendations expressed in this material are those of the authors and do not reflect the views of National Research Foundation, Singapore and the Civil Aviation Authority of Singapore.

REFERENCES

[1] Ludovica Adacher, Marta Flamini, and Elpidio Romano. Airport ground movement problem: minimization of delay and pollution emission. *IEEE Transactions on Intelligent Transportation Systems*, 19(12):3830–3839, 2018.

[2] Jason AD Atkin, Edmund K Burke, and Stefan Ravizza. The airport ground movement problem: Past and current research and future directions. In *Proceedings of the 4th international conference on research in air transportation (ICRAT), Budapest, Hungary*, pages 131–138, 2010.

[3] IBM ILOG Cplex. V12. 1: User's manual for cplex. *International Business Machines Corporation*, 46(53):157, 2009.

[4] Gurobi Optimization, LLC. Gurobi Optimizer Reference Manual, 2022.

[5] Yu Jiang, Xinxing Xu, Honghai Zhang, and Yuxiao Luo. Taxiing route scheduling between taxiway and runway in hub airport. *Mathematical Problems in Engineering*, 2015, 2015.

[6] Ellen Eun Kyoo Kim, Kwanglim Seo, and Youngjoon Choi. Compensatory travel post covid-19: Cognitive and emotional effects of risk perception. *Journal of Travel Research*, 61(8):1895–1909, 2022.

[7] Gammana Guruge Nadeesha Sandamali, Rong Su, Kalupahana Liyanage Kushan Sudheera, Yicheng Zhang, and Yi Zhang. Two-stage scalable air traffic flow management model under uncertainty. *IEEE Transactions on Intelligent Transportation Systems*, 22(12):7328–7340, 2020.

[8] Gammana Guruge Nadeesha Sandamali, Rong Su, and Yicheng Zhang. Flight routing and scheduling under departure and en route speed uncertainty. *IEEE Transactions on Intelligent Transportation Systems*, 21(5):1915–1928, 2019.

[9] Mojdeh Soltani, Sobhan Ahmadi, Ali Akgunduz, and Nadia Bhuiyan. An eco-friendly aircraft taxiing approach with collision and conflict avoidance. *Transportation Research Part C: Emerging Technologies*, 121:102872, 2020.

[10] ZHAI Wenpeng, LIU Runnan, and ZHU Chengyuan. Optimization of taxiway based on improved dijkstra algorithm. *Journal of Civil Aviation University of China*, 40(1):1, 2022.